SUPPLEMENTAL MATERIALS

SUPPLEMENTAL METHODS

Tumor analyses

Spontaneous tumor formation was monitored in 14 *Mob1a*$^{-/-}$*1b*$^{tr/+}$ and 23 *Mob1a*$^{-/+}$*1b*$^{tr/tr}$ mice. Mice were sacrificed when they became morbid (humane endpoint), making it difficult to determine the precise age of onset of each tumor. The mean ages of mice showing skin cancer, exostosis, osteosarcoma, fibrosarcoma, breast cancer, liver cancer, lung cancer, or salivary gland cancer were 50.7, 54.8, 52.7, 51.8, 51.0, 54.9, 60.0 and 41.0 weeks, respectively. Sections of tumors were cut for H&E staining, and DNA was extracted for Southern blotting. Skin cancer samples were also subjected to immunohistochemistry (IHC) and immunoblotting (see below).

Immunoblotting

Immunoblotting was carried out using a standard protocol and primary antibodies (Abs) recognizing: MOB1A/1B (1) for Figure 5; MOB1A/1B (Abgent) for Supplementary Figure 1D, Supplementary Figure 3; pLATS2 (T1041) (2); LATS2 (3); NF2, HES1 (Santa Cruz); pYAP1, YAP1, pLATS1(T1079), LATS1, pERK, ERK, pAKT, AKT, LEF1, α–Tubulin (all from Cell Signaling); GLI2 (4); Lamin (Abcam); or β-Actin (Sigma). Primary Abs were detected using HRP-conjugated secondary Abs (Cell Signaling).

siRNA

siRNA targeting of *Gli2* expression was performed using siRNA oligonucleotides directed against the sequence 5'-AAUGAUGCCAACCAGAACAAG-3'. Transfection of siRNA oligonucleotides (10 nM) into exponentially-growing keratinocytes at passage 4 was performed using Lipofectamine RNAiMAX (Invitrogen) following the manufacturer's protocol. At 48 h post-transfection, protein lysates were subjected to immunoblotting to detect GLI2 as described above.

Whole mount staining of inner ear structures

Inner ears of 25-week-old $Mob1a^{+/+}1b^{tr/tr}$ (control) and $Mob1a^{-/+}1b^{tr/tr}$ mutant mice were removed and organs of Corti were exposed by removing the stria vascularis. Tissues were fixed in 4% paraformaldehyde (PFA) in PBS, decalcified in 120 mM EDTA, blocked with 10% normal goat serum plus 1% BSA in PBS, and incubated overnight with anti-Myosin-6 Ab (Proteus). Immunostained tissues were then incubated for 1 hr with Alexa 568 anti-rabbit IgG (Invitrogen) and analyzed using a laser scanning confocal microscope (Bio Rad MRC 600, Philadelphia, PA, USA).

Histology and Immunohistochemistry

Freshly dissected skin samples were fixed in 4% PFA and embedded in paraffin using standard procedures. Sections (5 μm) were mounted on slides for standard histological or IHC analysis. IHC staining was performed using an indirect method employing primary Abs recognizing the following proteins: KRT15, KRT14, KRT5, Filaggrin (all from Covance); KRT17, SOX9 (Santa Cruz); Trichohyalin (Abcam); MOB1A/1B (Abgent); and Ki67 (Novocastra). Some slides were counter-stained with DAPI (Dojindo) or hematoxylin (for Ki67 detection) before mounting using PermaFluor (Thermo).

To detect GLI1 and GLI2, frozen skin sections (7 μm) were fixed in an ice-cold acetone:methanol solution for 2 min before immunostaining with anti-GLI1 or anti-GLI2 Ab (R&D). As a positive control for antibody staining, 293T cells were transfected with *pCMV-Gli1(ΔC; 1-260aa)* or *pCMV-Gli2(ΔN;134-424aa)* cDNA expression vectors.

TUNEL assays

Mouse skin samples were fixed with 2% PFA, stained with TUNEL using the *In situ* Cell Death Detection kit (Roche) according to the manufacturer's instructions, and counterstained with hematoxylin.

Flow cytometry

For surface marker detection, freshly isolated primary murine keratinocytes from *Mob1a/1b* double mutant and control mice at P19 were stained with biotin-conjugated anti-CD34 Ab (Pharmingen). Flow cytometric analyses were performed using a FACSCalibur™ (Becton Dickinson) and CellQuest Pro software.

Immunostaining of keratinocytes

Keratinocytes were isolated from mice at P4, and exponentially-growing cells at passage 4 were plated on coverslips and fixed for 5 min at -20^{o}C in methanol:acetone (1:1). To visualize centrosomes and microtubules, cells were incubated with primary anti-γ-Tubulin or anti-α-Tubulin Abs (Sigma), respectively, followed by incubation with secondary anti-rabbit/mouse IgG conjugated to Alexa Fluor 488 or 568 (Molecular Probes). Incubations were performed in PBS containing 2% normal goat serum as

described previously (5). DNA was stained using DAPI, and cells were examined using a BX51 microscope (Olympus) or a confocal laser-scanning microscope LSM510 (Zeiss). Over 200 mononucleated cells/mouse (n=6/group) were counted to analyze the percentage of cells with >2 centrosomes, and the percentage of cells with multiple nuclei. Over 100 mitotic cells/mouse (n=9/group) were counted to analyze the percentage of cells with a multipolar mitotic spindle.

Time-lapse video microscopy

Asynchronously grown keratinocytes were plated into 35-mm glass-base dishes (Iwaki) and maintained at 37°C using a stage heater on a model IX71 fluorescent microscope (Olympus) equipped with a humidity chamber and CO_2 injection control system. Images of cells passing through the four parts of mitosis were obtained using a high-sensitivity CoolSNAP-HQ CCD camera (Olympus), a Z-axis motor and 20x objective lens. Images were collected at 1 min intervals using MetaMorph imaging analysis software (Universal Imaging Ltd.). Over 100 mitotic cells were counted for each part of mitosis as defined in the main text.

Quantitative RT-PCR

Total RNA from freshly isolated primary keratinocytes from *Mob1a/1b* double mutant mice and control mice at P19, or *Mob1a/1b* double mutant ES cells and control ES cells, was extracted using RNAiso (TAKARA) according to the manufacturer's protocol. Total RNA (1 μg) was reverse-transcribed using the Transcriptor First Strand cDNA Synthesis Kit (Roche). Sequences of specific primer sets used for RT-PCR are listed in

the Supplementary Table 2. mRNA levels in the mutant were expressed as the percent increase over control values.

SUPPLEMENTAL REFERENCES

1. Hirabayashi S,et al. Threonine 74 of MOB1 is a putative key phosphorylation site by MST2 to form the scaffold to activate nuclear Dbf2-related kinase 1. *Oncogene* 2008; 27(31):4281-4292.
2. Zhang K, et al. Lats2 kinase potentiates Snail1 activity by promoting nuclear retention upon phosphorylation. *Embo J*. 2011; 31(1):29-43.
3. Yabuta N, Mukai S, Okada N, Aylon Y, Nojima H. The tumor suppressor Lats2 is pivotal in Aurora A and Aurora B signaling during mitosis. *Cell Cycle*. 2011; 10(16):2724-2736.
4. Cho A, Ko HW, Eggenschwiler JT. FKBP8 cell-autonomously controls neural tube patterning through a Gli2- and Kif3a-dependent mechanism. *Dev Biol*. 2008; 321(1):27-39.
5. Toji S, et al. The centrosomal protein Lats2 is a phosphorylation target of Aurora-A kinase. *Genes Cells* 2004; 9(5):383-397.

SUPPLEMENTAL FIGURE LEGENDS

Supplemental Figure 1. Targeting strategy and generation of Mob1a and Mob1b single mutant mice.

(A) Construction of the *Mob1a* targeting vector and mutant alleles. Top: The 4.7kb and 2.7 kb *Hin*dIII fragments diagnostic of the WT and targeted *Mob1a* alleles, respectively, are shown. WT allele: A portion of the mouse *Mob1a* WT locus showing the *Kpn*I (*K*) *Hin*dIII (*H*), and *Bam*HI (*B*) sites. Targeting vector: Targeting vector with the hygromycin resistance gene (Hyg^r) in reverse orientation to *Mob1a* transcription. Exon 2 was flanked by two *loxP* sequences (arrowheads), with a third *loxP* sequence flanking Hyg^r. Targeted allele: The mutated $Mob1a^{ta}$ allele containing three *loxP* sequences and the Hyg^r gene. Flox allele: $Mob1a^{flox}$ allele produced after Cre-mediated Hyg^r deletion. *Δ* allele: $Mob1a^{\Delta}$ allele produced after Cre-mediated deletion. Bottom: The 9.1kb, 6.5kb, and 4.7kb *Kpn*I fragments diagnostic of the *WT Mob1a* allele, the $Mob1a^{flox}$ allele and $Mob1a^{\Delta}$ allele, respectively, are shown. The 5'-flanking probe (Probe A) and a 3' long arm probe (Probe B) are also indicated.

(B) Gene trap mutation of *Mob1b*. WT allele: A portion of the mouse *Mob1b* WT locus showing the *Hin*dIII (*H)* and *Eco*RV (*EV*) sites. The 6.0 kb *Eco*RV fragment diagnostic of the WT allele is indicated. Trapping vector: Trapping vector showing *β-geo* and splice acceptor (SA) site. A single copy of the targeting vector was inserted into intron 1 of *Mob1b*. Trapped allele: Mutated *Mob1b* locus, with its diagnostic 7.5 kb *Eco*RV fragment. The 5'-flanking probe (Probe C) is also shown.

(C) Left panels: Southern blot of *Hin*dIII-digested (left blot) or *Bam*HI-digested (right blot) genomic DNA from ES cells of genotype $Mob1a^{+/+}$ (left lane of each blot), or ES

cells bearing the mutated *Mob1a* allele containing three *loxP* sequences and the Hyg^r gene (right lane of each blot). Right panels: Southern blot of *Eco*RV-digested (left blot) or *Hin*dIII-digested (right blot) genomic DNA from ES cells of genotype $Mob1b^{+/+}$ (left lane), or ES cells bearing the *Mob1b* gene trap allele (right lane). The probe [from (A) or (B)] used for hybridization in each case is indicated above the lane.

(D) Confirmation of *Mob1* deletion. Mouse keratinocytes were isolated from mice of the indicated genotypes and infected (+) or not (-) with Cre-expressing adenovirus. Extracts were subjected to standard immunoblotting to detect MOB1. β-Actin, loading control.

(E) Gross appearance (left) and body weight (right) of representative 12-week-old mice of the indicated genotypes. No obvious abnormalities were observed in *Mob1a* or *Mob1b* single mutant mice. Body weight data are the mean ± SEM (n=5/group).

Supplemental Figure 2. Non-cancerous phenotypes observed in Mob1 mutant mice.

(A) Severe (left) and mild (right) dental malocclusion in $Mob1a^{\Delta/+}1b^{tr/tr}$ mice. (B) Immunohistochemical analysis using anti-Myosin-6 Ab to visualize the disorganized hair bundles in a $Mob1a^{\Delta/+}1b^{tr/tr}$ mutant mouse compared to a control ($Mob1a^{+/+}1b^{tr/tr}$) mouse. Scale bar, 50 μm. (C) H&E-stained sections of femoral bone tissue showing an increased number of trabeculae in a $Mob1a^{\Delta/+}1b^{tr/tr}$ mouse compared to a control. Bar, 1000 μm. The phenotypes of (A)-(C) were also observed in $Mob1a^{\Delta/\Delta}1b^{tr/+}$ mice.

Supplemental Figure 3. Confirmation of Mob1a/1b deletion in keratinocyte-specific Mob1a/1b double homozygous mutant (kDKO) mice.

(A) Southern blot of *Kpn*I-digested genomic DNA from $Krt14CreERMob1a^{fl/fl}1b^{tr/tr}$

keratinocytes with/without tamoxifen treatment. Tamoxifen was administered intraperitoneally to 1-day-old mice (P1; 0.2 mg), and Southern blotting of keratinocytes was performed at 16 days post-injection. Hybridization was performed using Probe B (see Supplemental Figure 1A).

(B) Immunoblot to detect MOB1A/1B in keratinocytes from *Mob1a*$^{+/+}$*1b*$^{+/+}$ (wild type), *Mob1a*$^{+/+}$*1b*$^{tr/tr}$, and *k*DKO(P1) mice at P17. β-Actin, loading control.

(C) Immunostaining to detect MOB1A/1B in fat pad epidermis and back skin from *Mob1a*$^{+/+}$*1b*$^{+/+}$ (wild type) and *k*DKO(P1) mice. Bars, 50 μm.

(D) Immunostaining to detect MOB1A/1B in IFE and head HF from human non-tumorous tissue. Bars, 50 μm.

Supplemental Figure 4. HF and IFE hyperplasia in kDKO(P1) mice.

Representative histological analyses of H&E-stained skin sections from control (without tamoxifen) and *k*DKO(P1) mice sacrificed on the indicated day after birth. The middle and right columns of panels are higher magnification images of the left column of panels. Bar, 400 μm (left columns); 40 μm (middle columns); 100 μm (right columns). Data are representative of more than 10 mice/group/sacrifice day.

Supplemental Figure 5. Immunohistochemical confirmation of altered IFE in back skin of kDKO(P1) mice.

Tissues from control and *k*DKO(P1) mice at P16 were immunostained with fluorescent Abs recognizing the indicated skin markers, eg. KRT15. Data are representative of more than 5 mice/group. Bar, 50 μm.

Supplemental Figure 6. Decreased survival of kDKO(P28) mice.

Kaplan-Meier analysis of *k*DKO(P28) mice (n=20) administered tamoxifen (0.5 mg/day) for 7 days on days 28-34 after birth. *Krt14CreERMob1a*$^{fl/fl}$*1b*$^{tr/tr}$ mice without tamoxifen (n=10) and *Mob1a*$^{fl/fl}$*1b*$^{tr/tr}$ mice with tamoxifen treatment (n=10) were used as controls (shown jointly). All 20 *k*DKO(P28) mice were dead within 52 days after tamoxifen administration.

Supplemental Figure 7. Abnormalities in MEFs lacking Mob1.

Top: MEFs derived from control and *k*DKO(P1) mice were immunostained with anti-γ-Tubulin, anti-α-Tubulin or DAPI to detect (A) centrosomes, (B) mitotic spindles, or (C) micronuclei, respectively. Mutant cultures showed increased numbers of cells with excessive numbers of centrosomes, multi-polar spindles, and cytoplasmic micronuclei. Bar, 10 μm for A; 20 μm for B,C. For (A, C), over 240 mononucleated cells were counted. For (B), over 120 mitotic cells were counted. Bottom: Quantitation. Data shown are the mean ± SEM; *p<0.01.

Supplemental Figure 8. Loss of Mob1 leads to accelerated exit from mitosis.

(A) Duration of four morphological parts of mitosis (as defined in the main text) analyzed in control and *k*DKO(P1) keratinocytes. Data are the mean ± SEM; *p<0.01.

(B) Time-lapse DIC (differential interference contrast) images of morphological parts I and IV of mitosis in control and *k*DKO(P1) keratinocytes. Images were captured at 1 min intervals and are representative of over 100 mitotic cells examined per group. White arrows indicate the start of each mitotic phase, while yellow arrows indicate the end.

Supplemental Figure 9. Immunostaining of HF bulge stem cells.

Representative immunohistochemical analysis using anti-CD34 (green) and anti-SMA (red) Abs to identify HF bulge stem cells and the arrector pili muscle, respectively, in back skin of control and kDKO(P1) mice at P19. Data are representative of 6 mice/genotype. Bar, 50 μm

Supplemental Figure 10. The SHH pathway is not obviously activated in the absence of Mob1a/1b.

(A) 293T cells were transfected with vector expressing murine *Gli1* (1-260 aa) cDNA (top), or murine *Gli2* (134-424 aa) cDNA (bottom), and immunostained with anti-GLI1 or anti-GLI2 Ab. Bar, 20 μm.

(B) Immunostaining of the back skin of a wild type (control) mouse embryo (E18.5) using the same anti-GLI1 or anti-GLI2 Abs (green) as in (A). Tissues were counterstained with anti-α6-integrin Ab (red) to visualize the basement membrane. Bars, 50 μm.

(C) Immunostaining to detect murine GLI1 in the back skin of control and *k*DKO(P1) mice at P19. Data are representative of 5 mice/genotype. Bars, 50 μm.

A ***Supplementary Movie*** is available on-line that shows a $Mob1a^{-/+}1b^{tr/tr}$ mouse (white) exhibiting disequilibrium, tilting its head to one side, and failing to walk in a straight line, in contrast to a control $Mob1a^{-/+}1b^{tr/+}$ mouse (black).

SUPPLEMENTAL TABLES

Supplementary Table 1
Genotypes of neonates from Mob1a$^{\Delta/+}$1b$^{tr/+}$ intercrosses

		Mob1b		
		+/+	*tr/+*	*tr/tr*
Mob1a	*+/+*	49	105	54
	Δ/+	77	189	97
	Δ/Δ	47	54	0

Total 672 pups

Genotypes were determined by Southern blotting using probes A and C shown in Supplemental Figure 1A, B.

Supplementary Table 2

Primer Sequences

1. Primer sets for genotyping by PCR
(1) *Mob1a* wild type and *Mob1a*^{flox} alleles
5'- CTCTAGCTGTAGAGAATCCAGCAG -3'
5'- CCTGGTTGGGGTGGAGAATCAAG -3'
WT:319 bp and floxed:470bp products
(2) *Mob1a*$^{\Delta}$ allele
5'- GTAATGTGTTCAGCTATGCTTTGAC -3'
5'- CCTGGTTGGGGTGGAGAATCAAG -3'
551 bp product
(3)*Mob1b* wild type allele
5'- CTTCAGGATCCTTGGTGGTTATCAG -3'
5'- AGAGCAAGGGGAAAAGAAGCTCAATG -3'
586 bp product
(4)*Mob1b*^{trap} allele
5'- CTTCAGGATCCTTGGTGGTTATCAG -3'
5'- TCAGGGTCACAAGGTTCATATGGTG -3'
673 bp product
(5) *Krt14CreER allele*
5'- GCGGTCTGGCAGTAAAAACTATC -3'
5'- GTGAAACAGCATTGCTGTCACTT -3'
100 bp product
2. Primer sets for quantitative RT-PCR
(1) *Cdx2*
5'- AAACCTGTGCGAGTGGATG -3'
5'- GCTGATGGTCTGTGTACACC -3'
104 bp product
(2) *Eomesodermin*
5'- CACCTTCTCAGAGACACA -3'
5'- TCTGATGGGATGAATCGTAG -3'
125 bp product
(3) *Oct3/4*
5'- CTCCTCTGAGCCCTGTGCCGA -3'

5’- CTGCAAGGCCTCGAAGCGACA -3’
238 bp product
(4) *Sall4*
5’- CCAATGCGCGCACCATGTCG -3’
5’- GGCCGCTTCACCGGTATGGA -3’
199 bp product
(5) *Nanog*
5’- TTGCTTACAAGGGTCTGCTACT -3’
5’- ACTGGTAGAAGAATCAGGGCT -3’
106 bp product)
(6) *Fgf5*
5’- GCTCCCACGAAGCCAGTGTGT -3’
5’- GTTCTGTGGATCGCGGACGCA -3’
211 bp product
(7) *Pax6*
5’- GGCGGAGTTATGATACCTACAC -3’
5’- ATCGAGGCCAGTACTGAGAC -3’
165 bp product
(8) *Sox2*
5’-GCGGAGTGGAAACTTTTGTCC-3’
5’-CGGGAAGCGTGTACTTATCCTT-3’
157 bp product
(9) *Pdgfra*
5’- TCCATGCTAGACTCAGAAGTCA -3’
5’- TCCCGGTGGACACAATTTTTC -3’
140 bp product
(10) *Gata4*
5’- CACCCCAATCTCGATATGTTTGA -3’
5’- GGTTGATGCCGTTCATCTTGT -3’
151 bp product
(11) *β-Actin*
5’- GGCTGTATTCCCCTCCATCG -3’
5’- CCAGTTGGTAACAATGCCATGT -3’
154 bp product
(12) *Sox9*

5’- AAGAACAAGCCACACGTCAA -3’
5’- TCTCTTCTCGCTCTCGTTCA -3’
159 bp product
(13) *Lgr5*
5’- TTTCAGCGGCCTGCACTCCC -3’
5’- GGAGATGCAGAACCACGAGGCTG -3’
182 bp product
(14) *Cd34*
5’- TACCACGGAGACTTCTACACAAG -3’
5’- TGGAGTTCCAGAGCCTGAA -3’
202 bp product
(15) *Lgr6*
5’- GGCTGGATGACAATGCACTCAC -3’
5’- AGATTGTGCAGCCCCTCGAA -3’
205 bp product

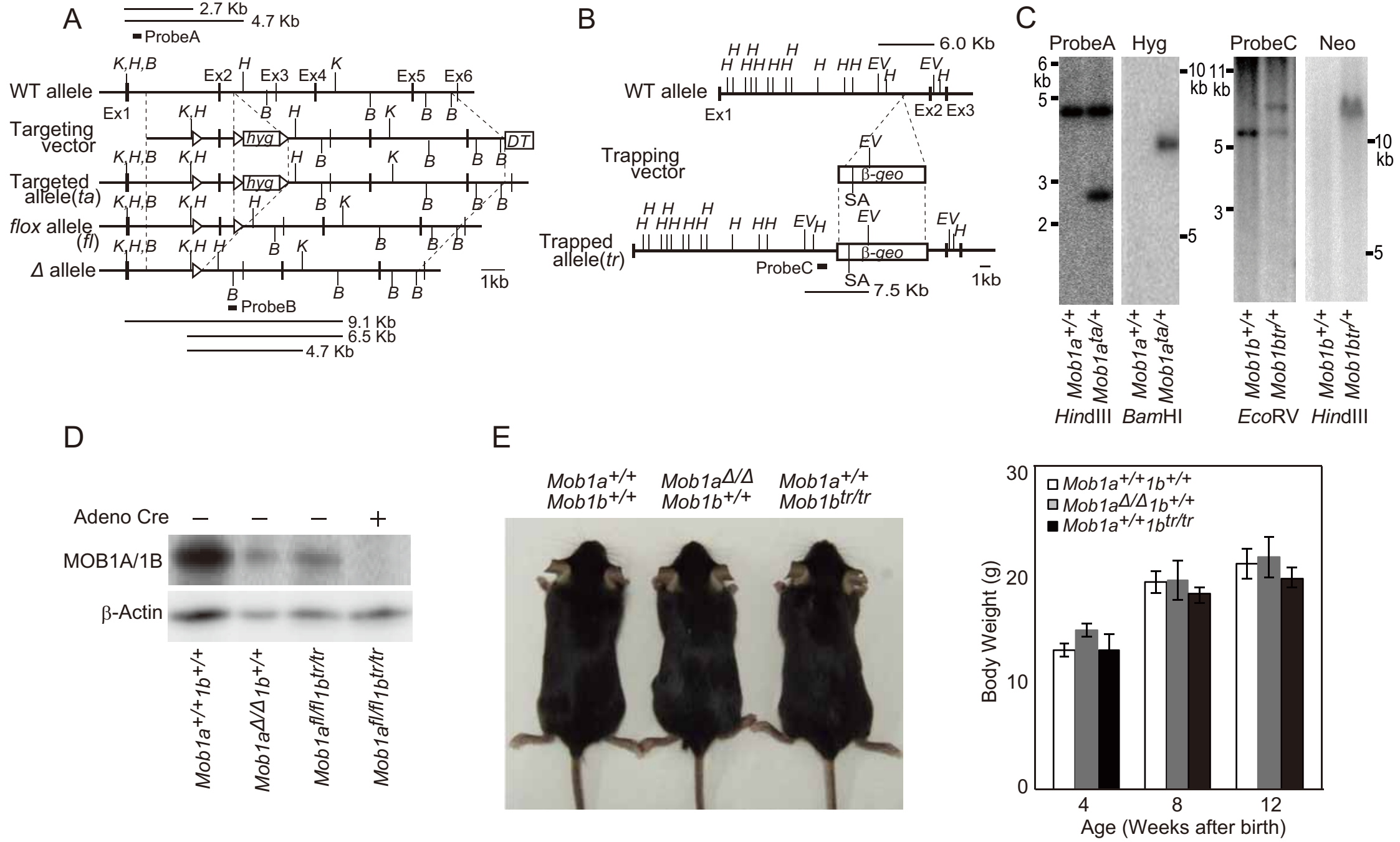

Supplemental Figure1. Nishio et al.

A

B

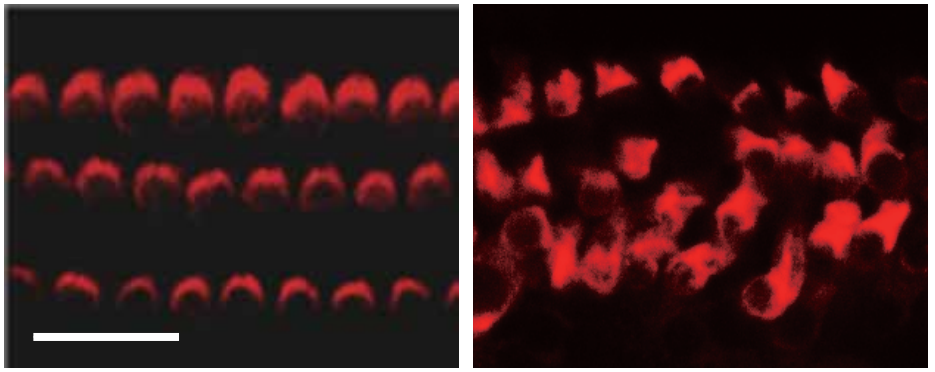

C

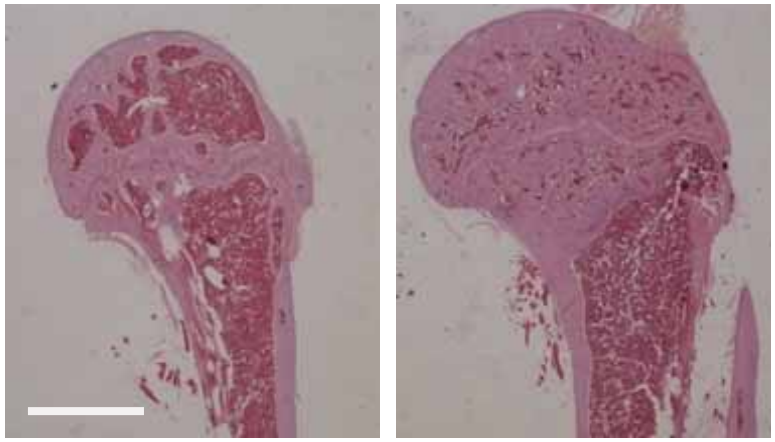

Supplemental Figure 2. Nishio et al.

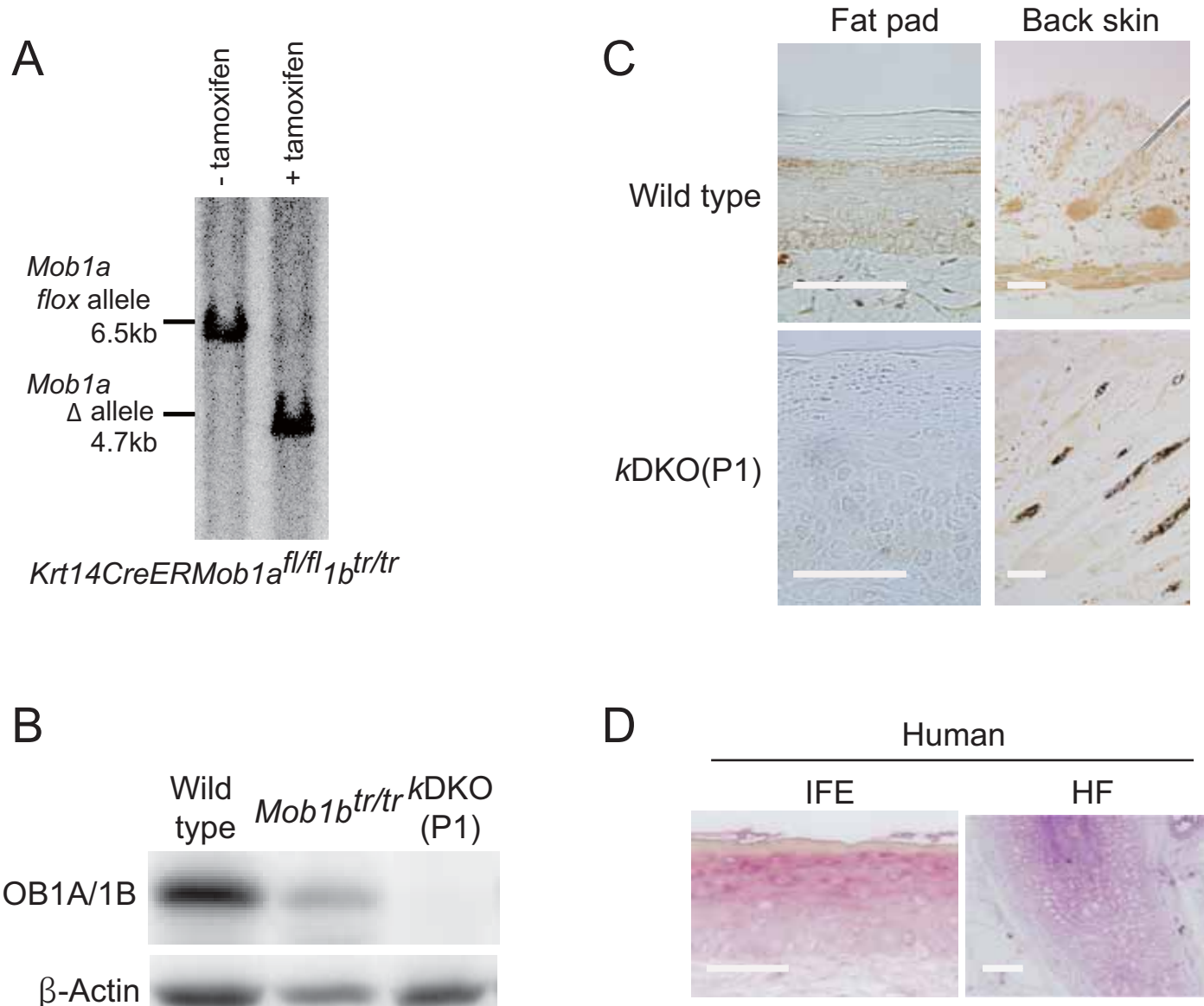

Supplemental Figure 3. Nishio et al.

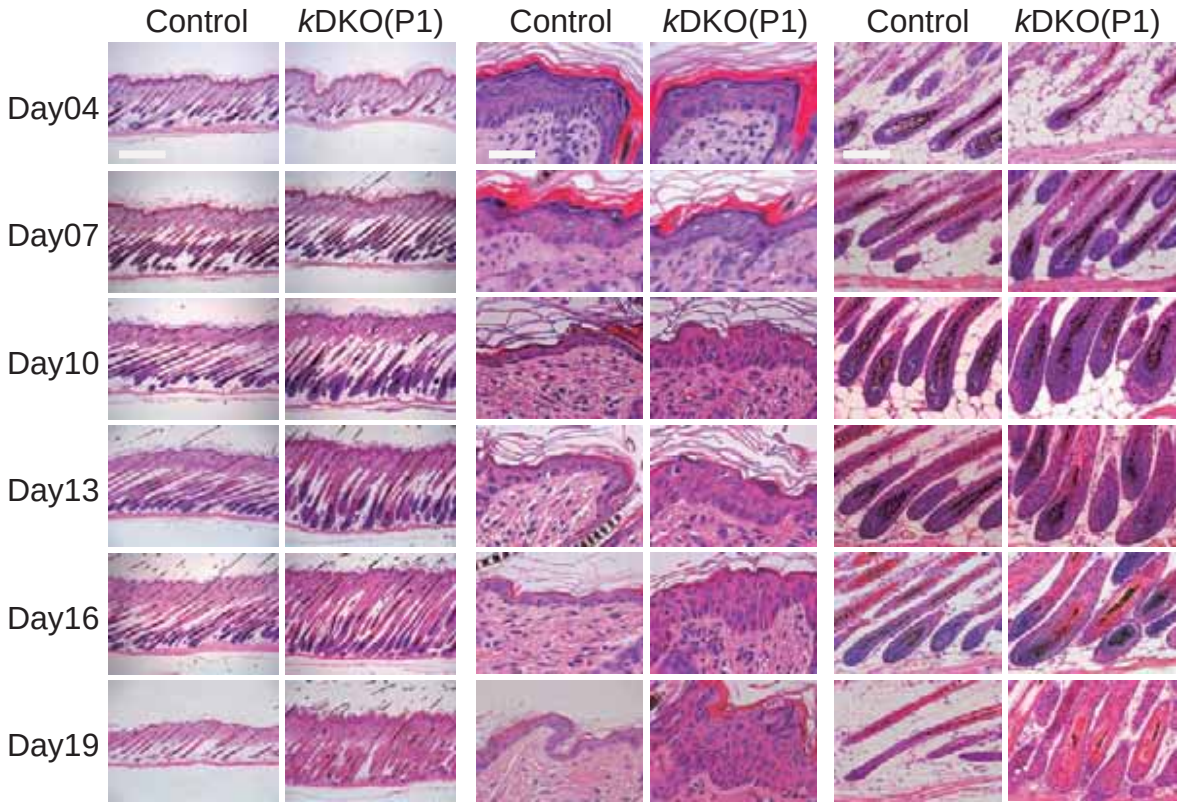

Supplemental Figure 4. Nishio et al.

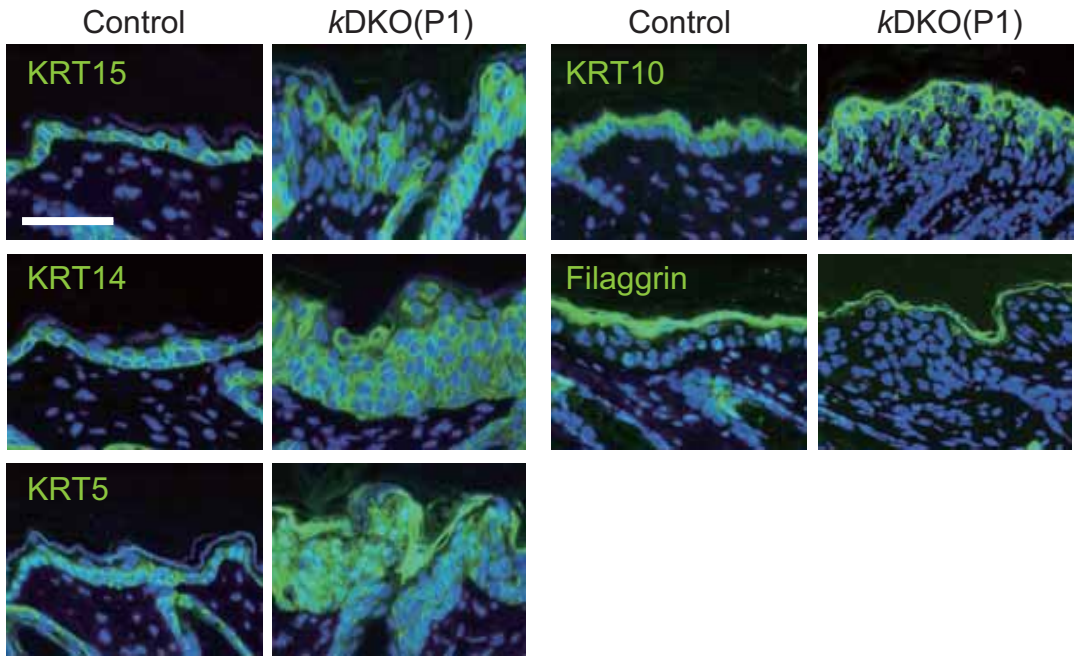

Supplemental Figure 5. Nishio et al.

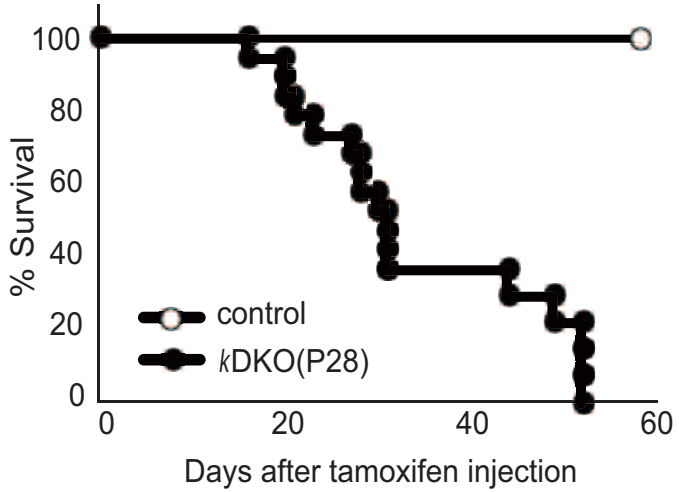

Supplemental Figure 6. Nishio et al.

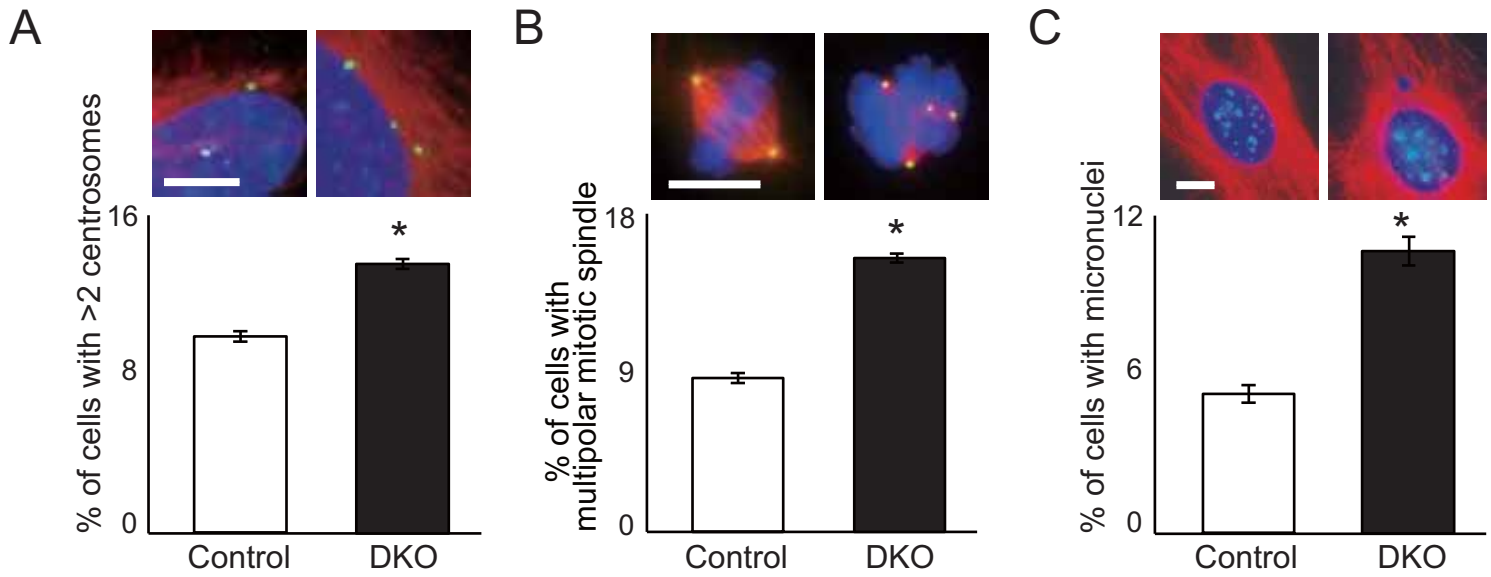

Supplemental Figure 7. Nishio et al.

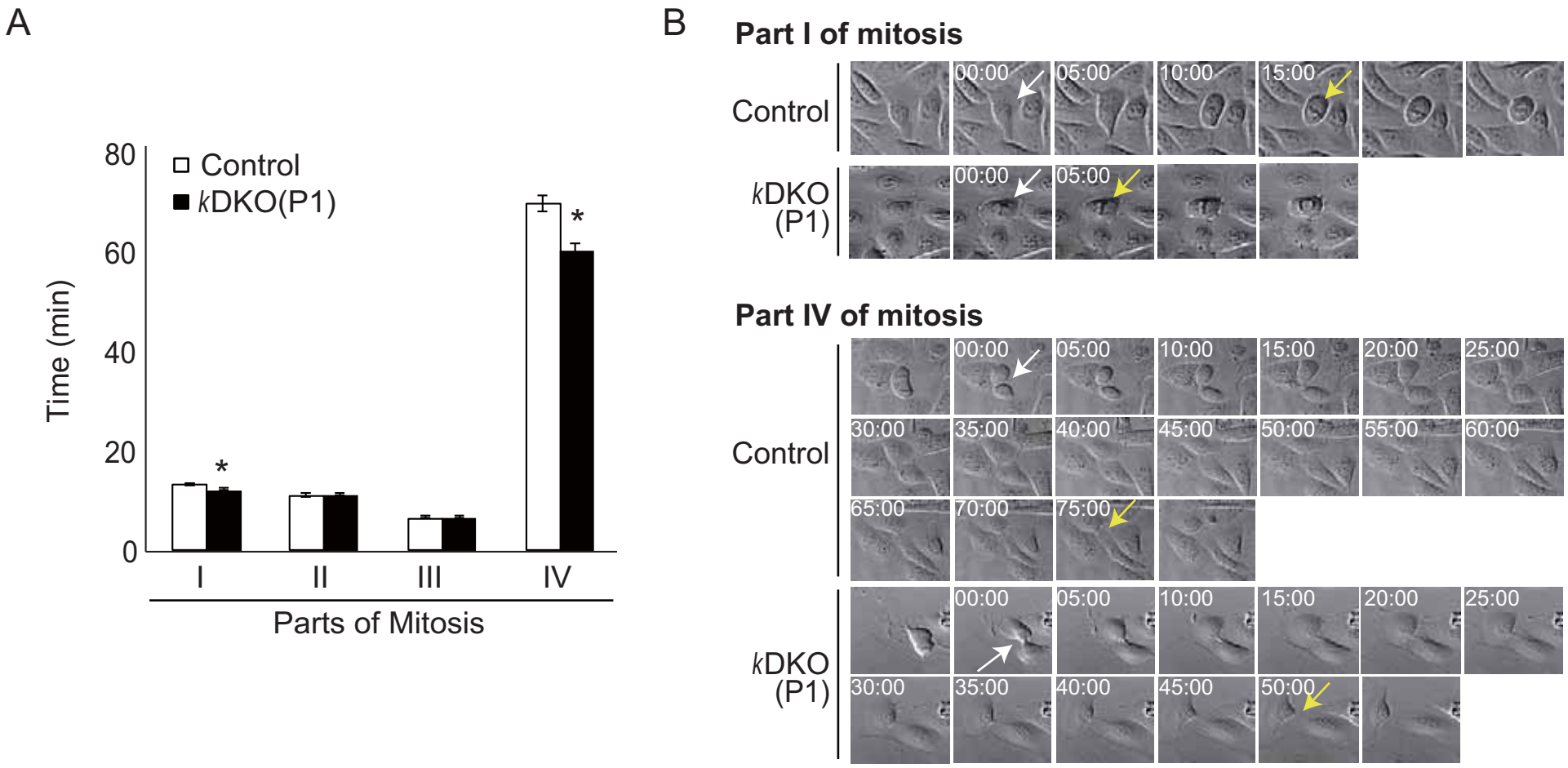

Supplemental Figure 8. Nishio et al.

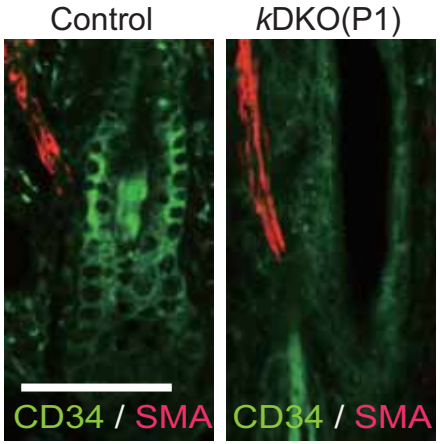

Supplemental Figure 9. Nishio et al.

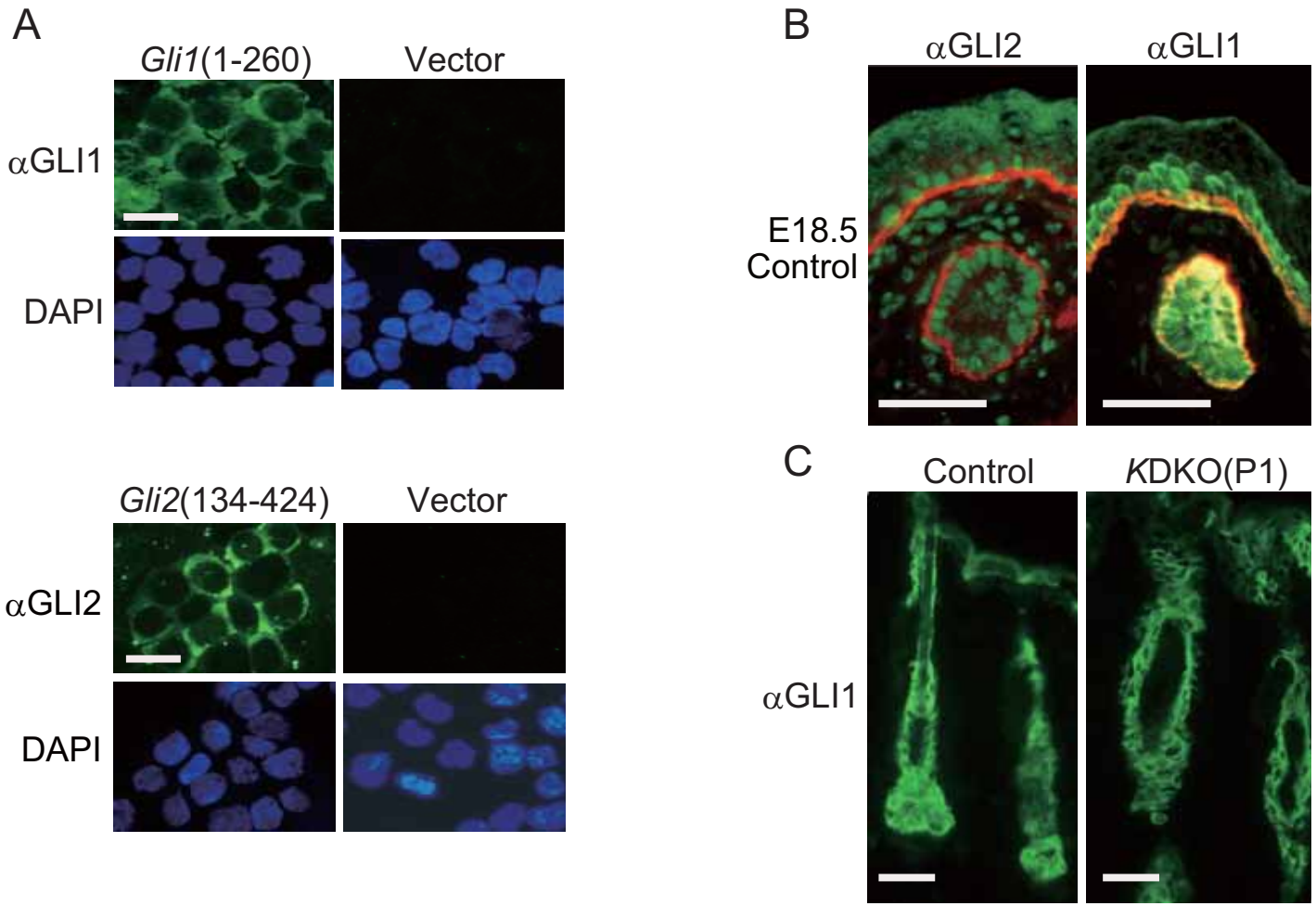

Supplemental Figure 10. Nishio et al.